SOCAR Proceedings Special Issue 1 (2022) 016-022

SOCAR Proceedings

Oil and gas structures and equipment

journal home page: http://proceedings.socar.az

ON THE TORSIONAL BUCKLING MOMENT OF CYLINDRICAL SHELLS CONSISTING OF FUNCTIONALLY GRADED MATERIALS RESTING ON THE PASTERNAK-TYPE SOIL

A. H. Sofiyev[1,5]*, F. Kadioglu[2], I. A. Khalilov[3], H. M. Sedighi[4], T. Vergul[2,6], R. Yenialp[1]

[1]*Suleyman Demirel University, Isparta;* [2]*Istanbul Technical University, Istanbul, Turkey;*
[3]*Azerbaijan Technical University, Baku, Azerbaijan;* [4]*Shahid Chamran University of Ahvaz, Ahvaz, Iran;*
[5]*UNEC Azerbaijan State Economics University, Baku, Azerbaijan;* [6]*Istanbul Ticaret University, Istanbul,Turkey*

A B S T R A C T

In this study, the buckling analysis of cylindrical shells made of functionally graded materials (FGMs) under the torsional moment resting on the Pasternak-type soil is performed. After establishing the linear constitutive relations of FGM cylindrical shells within the framework of the modified Donnell type shell theory, the governing equations of FGM cylindrical shells under the torsional moment are derived considering the influence of Pasternak-type soil. Analytical formula for the torsional moment is obtained by choosing the approximation functions that satisfies the boundary conditions in an integral sense. From the obtained formula, the formulas for the critical torsional moment in the presence of Winkler soil and absence of soils are obtained as a special case. Variations of critical torsional moment for different soil coefficients, volume fraction ratio and shell characteristics are investigated in detail.

K E Y W O R D S

Functionally graded materials;
Cylindrical shell;
Buckling;
Critical torsional moment;
Pasternak-type soil.

1. Introduction

In recent years, functionally graded materials (FGMs) as a new generation composite material class have received great attention in industries such as construction, machinery, aerospace and transportation due to their superior mechanical properties. The use of new generation heterogeneous composites resistant to corrosion, radiation, humidity and similar factors is in demand in advanced technologies, since the properties of cylindrical pipes made of traditional materials used in oil and gas pipelines make their use insufficient in various climatic regions. Among such heterogeneous composites, FGMs have an important place in applications due to their superior properties. Functionally graded materials have been proposed by a group of materials scientists in Japan as an alternative to laminated composite materials that exhibit incompatibility in properties at material interfaces [1]. Since then, FGMs have been the focus of attention of both the academic and engineering communities for their outstanding advantages, such as the potential reduction of in-plane and transverse stresses throughout the thickness, improved residual stress distribution, improved thermal properties, higher fracture toughness, and resistance to corrosion and moisture [2,3]. Several studies on various aspects of FCMs have been published over the years [4-10].

FGM cylindrical shells are one of the most commonly used structural elements in severe operating conditions, including fusion reactors, storage tanks, pressure vessels, general wear and corrosion resistant coatings in the aerospace and engine industries. Therefore, buckling analysis of cylindrical shells made of FGMs under torsion are very important for practical applications. Analytical and numerical solutions on the torsion problems of FGM circular shells have attracted the attention of many researchers because the cylindrical shells have high torsional strength and stiffness, and this interest still continues [11-17]. Comprehensive information on the formation of FGMs, their superior thermal and mechanical properties, applications, and static and dynamic behavior of shells can be found in book of Shen [18].

As structural members made of FGMs are used in a variety of environments (tunnels, storage tanks, pressure vessels, water channels, pipelines and containment pipes, process equipment, and other applications), the effects of elastic environments on their behavior are critical to safety. One of the more frequently used models that better describe the structure of elastic soils is the Pasternak elastic soil model [19]. The special case of this soil model is the Winkler elastic soil model, which is defined as a system of parallel springs that do not touch each other [20-22]. In recent years, some studies on the buckling analysis of FGM cylindrical shells resting on different elastic foundations have been published in the literature [23-29].

Considering the material gradient effects, the complexity of the buckling problem of shells subjected to torsional moment increases significantly. Furthermore, the solution of buckling problems of circular shells under the torsional moment in the presence of soils is more complicated than with other compressive loads, for example, axial, external and hydrostatic pressure loads. Therefore, the buckling problem of FGM cylindrical shells resting on the Pasternak-type elastic soils under the torsional moment is less explored compared to other loadings. The literature review reveals that

***E-mail:** abdullahavey@sdu.edu.tr
http://dx.doi.org/10.5510/OGP2022SI100695

the buckling of FGM cylindrical shells resting on Pasternak-type soils and subjected to torsional moments has not been investigated sufficiently yet. In this study, an attempt is made to solve this problem.

2. Formulation of problem

The cylindrical shell with thickness, radius and length, which is formed from the FGM presented in fig. 1, is on a Pasternak-type elastic ground and is subjected to torsional moment from the sides. The *Oxyz* coordinate system has been chosen at the midpoint of the middle surface of the shell and the *Ox* axis is in the main direction, the *Oy* axis is in the circumferential direction, and the *Oz* axis is normal to the surface where the other two axes are located and directed inwards (fig. 1). In the chosen coordinate system, the shallow shells are defined as the three-dimensional region Γ, as follows:

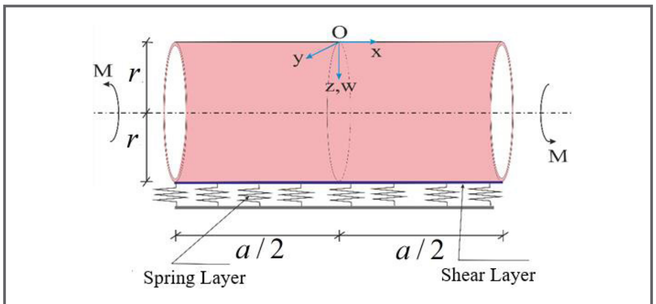

Fig. 1. The cylindrical shell consisting of FGM resting on Pasternak-type elastic ground under torsional moment and its coordinate system

$$\Gamma = \left\{x, y, z : (x, y, z) \in [0, a]\times[0, 2\pi r]\times[-t/2, t/2]\right\} \tag{1}$$

The mathematical expression of the Pasternak-type elastic soil model is as follows [20-22]:

$$N = K_1 w - K_2(w_{,xx} + w_{,yy}) \tag{2}$$

where, (,) shows the partial derivative with respect to the coordinate, w is the deflection in the z direction, N is the reaction force per unit area of the Pasternak-type soil, K_1 (in N/m^3) is the base reaction coefficient of the elastic soil, K_2 (in N/m) is the shear modulus of the elastic soil, and it is the inwardly directed displacement in the normal direction to the reference surface, which is much smaller than the cylinder thickness. As can be seen from the equation (2), if $K_2 = 0$, the model of the two-parameter elastic soil transforms into the Winkler elastic soil model (fig. 1).

The effective properties of FGMs, namely the effective Young's modulus $E^{Fd}(Z)$ and the effective Poisson's ratio $\upsilon^{Fd}(Z)$, are expressed by power function as follows [18]:

$$\begin{gathered} E^{Fd}(Z) = E^m + (E^c - E^m)V^c, \quad \upsilon^{Fd}(Z) = \upsilon^m + (\upsilon^c - \upsilon^m)V^c, \\ V^c = (Z + 0.5)^k, \quad V^c + V^m = 1 \end{gathered} \tag{3}$$

where, the elastic properties of the ceramic and metal surfaces of the FGM are denoted by E^c and E^m, V^c and V^m are the ceramic and metal volume fractions, respectively and k is the volume fraction index, a non-negative number that describes the material distribution..

3. Governing equations

Considering the Kirchoff-Love assumption, the basic relations of cylindrical shells composed of FGMs can be expressed as follows [11]:

$$\begin{bmatrix} \sigma_{11} \\ \sigma_{22} \\ \sigma_{12} \end{bmatrix} = \begin{bmatrix} Q_{11} & Q_{12} & 0 \\ Q_{12} & Q_{11} & 0 \\ 0 & 0 & Q_{12} \end{bmatrix} \begin{bmatrix} e_{11} - zw_{,xx} \\ e_{22} - zw_{,yy} \\ e_{12} - zw_{,xy} \end{bmatrix} \tag{4}$$

where, σ_{ij} (i, j=1, 2) are stress components, e_{ij} (i, j=1, 2) are strain components on the mid-surface and Q_{ij} (i, j=1, 2, 6) are coefficients depending on the properties of cylindrical shells composed of FGMs and are defined as follows:

$$Q_{11} = \frac{E^{Fd}(Z)}{1 - \left[\upsilon^{Fd}(Z)\right]^2}, \quad Q_{12} = \frac{\upsilon^{Fd}(Z)E^{Fd}(Z)}{1 - \left[\upsilon^{Fd}(Z)\right]^2}, \quad Q_{66} = \frac{E^{Fd}(Z)}{1 + \upsilon^{Fd}(Z)} \tag{5}$$

The following relationship is used between the $[N_{11}, N_{22}, N_{12}]$ force components and the Airy stress function, [30]:

$$\left[N_{11}, N_{22}, N_{12}\right] = t\left[\Phi_{,yy}, \Phi_{,xx}, \Phi_{,xy}\right] \tag{6}$$

The strain components on the mid-surface and moment components of the cylindrical shells produced from FGM are expressed as the stress function and curvature changes in the mid-surface as follows:

$$\begin{bmatrix} e_{11} \\ e_{22} \\ e_{12} \end{bmatrix} = \begin{bmatrix} b_{11}t\Phi_{,yy} + b_{12}t\Phi_{,xx} - b_{13}w_{,xx} - b_{14}w_{,yy} \\ b_{12}t\Phi_{,yy} + b_{11}t\Phi_{,xx} - b_{13}w_{,xx} - b_{14}w_{,yy} \\ -b_{31}t\Phi_{,xy} - b_{32}w_{,xy} \end{bmatrix} \tag{7}$$

$$\begin{bmatrix} M_{11} \\ M_{22} \\ M_{12} \end{bmatrix} = \begin{bmatrix} c_{11}h\Phi_{,yy} + c_{12}h\Phi_{,xx} - c_{13}w_{,xx} - c_{14}w_{,yy} \\ c_{12}h\Phi_{,yy} + c_{11}h\Phi_{,xx} - c_{13}w_{,xx} - c_{14}w_{,yy} \\ -c_{31}h\Phi_{,xy} - c_{32}w_{,xy} \end{bmatrix} \tag{8}$$

where

$$\begin{gathered} c_{11} = a_{111}b_{11} + a_{121}b_{12}, \quad c_{12} = a_{111}b_{12} + a_{121}b_{11}, \\ c_{13} = a_{111}b_{13} + a_{121}b_{11} + a_{112}, \quad c_{14} = a_{111}b_{14} + a_{121}b_{13} + a_{122}, \\ c_{31} = a_{661}b_{61}, \quad c_{32} = a_{661}b_{62} + a_{662}, \quad b_{11} = a_{110}/\Delta, \\ b_{12} = a_{120}/\Delta, \quad b_{13} = (a_{120}a_{121} - a_{111}a_{110})/\Delta, \\ b_{14} = (a_{120}a_{111} - a_{121}a_{110})/\Delta, \quad b_{31} = 1/a_{660}, \\ b_{32} = -a_{661}/a_{660}, \quad \Delta = (a_{110}^2 - a_{120}^2), \\ a_{11i} = \int_{-t/2}^{t/2} \frac{E^{Fd}(Z)}{1 - \left[\upsilon^{Fd}(Z)\right]^2}dz, \quad a_{12i} = \int_{-t/2}^{t/2} \frac{\upsilon^{Fd}(Z)E^{Fd}(Z)}{1 - \left[\upsilon^{Fd}(Z)\right]^2}dz, \\ a_{66i} = \int_{-t/2}^{t/2} \frac{E^{Fd}(Z)}{2\left[1 + \upsilon^{Fd}(Z)\right]^2}dz (i = 0.1, 2) \end{gathered} \tag{9}$$

The general stability equations of cylindrical shells on the Pasternak-type elastic foundation are obtained by applying Hamilton's principle as follows [30]:

$$\begin{gathered} M_{11,xx} + 2M_{12,xy} + M_{22,yy} + N_{22}/r + N_{11}^0 w_{,xx} + 2N_{12}^0 w_{,xy} + \\ + N_{22}^0 w_{,yy} - K_1 w + K_2(w_{,xx} + w_{,yy}) = 0 \end{gathered} \tag{10}$$

$$e_{11,yy} + e_{22,xx} - 2e_{12,xy} = -w_{,xx}/r \tag{11}$$

When the equations (6)-(8) are substituted into (10) and (11), after mathematical operations, the stability and deformation compatibility equations of the cylindrical shells composed of FGMs resting on the Pasternak-type elastic soil under torsional moment, transform into the following partial differential equations:

$$\begin{gathered} t\left[c_{12}\Phi_{,xxxx} + 2(c_{12} - c_{31})\Phi_{,xxyy} + c_{12}\Phi_{,yyyy} + \frac{\Phi_{,xx}}{r}\right] - c_{13}w_{,xxxx} - \\ -2(c_{14} + c_{32})w_{,xxyy} - c_{13}w_{,yyyy} + \frac{w_{,xx}}{r} - \frac{M}{\pi r^2}w_{,xy} - \\ -K_1 w + K_2(w_{,xx} + w_{,yy}) = 0 \end{gathered} \tag{12}$$

$$t\left[b_{11}\Phi_{,xxxx}+2(b_{12}+b_{31})\Phi_{,xxyy}+b_{11}\Phi_{,yyyy}\right]-b_{14}w_{,xxxx}-$$
$$-2(b_{13}-b_{32})w_{,xxyy}-b_{14}w_{,yy}+\frac{1}{r}w_{,xx}=0 \qquad (13)$$

4. Solution of governing equations

In the case of torsion, it is assumed that the buckling of the cylindrical shell will be accompanied by the formation of waves regularly located in the circumference, inclined at a known angle to the x direction of the cylindrical shell. Therefore, the deflection and Airy stress functions are sought as follows [11,30]:

$$w=0.5A_1\left\{\cos\frac{n[y+(q-\lambda)x]}{r}-\cos\frac{n[y+(q+\lambda)x]}{r}\right\}$$
$$w=0.5A_2\left\{\cos\frac{n[y+(q-\lambda)x]}{r}-\cos\frac{n[y+(q+\lambda)x]}{r}\right\} \qquad (14)$$

where, $\lambda=(\pi r)/(na)$, n is the number of waves in the circumference, q is the tangent of the angle formed by the waves with the x axis, A_1 and A_2 are the unknown amplitudes of the deflection and Airy stress functions, respectively.

The approximation functions (14) satisfy the boundary conditions at $x=\pm0.5$ in integral sense:

$$\int_0^{2\pi r} w_{,x}\Big|_{x=\pm0.5a}dy=\int_0^{2\pi r} w_{,xx}\Big|_{x=\pm0.5a}dy=0,$$
$$\int_0^{2\pi r} \Phi_{,x}\Big|_{x=\pm0.5a}dy=\int_0^{2\pi r} \Phi_{,xx}\Big|_{x=\pm0.5a}dy=0 \qquad (15)$$

Let's apply the Galerkin method by multiplying the equations (12) and (13), by the weight function in the region $\Lambda=\{(x,y): -0.5a\le x\le 0.5a,\ 0\le y\le 2\pi r\}$, and after the integration, the amplitude is eliminated, giving the following expression for the critical torsional moment of the FGM cylindrical shells on the Pasternak-type elastic soil:

$$M_{kr}=\frac{\pi}{n^2q}\left\{\begin{bmatrix} r(q^2n^2+\eta^2)-c_{12}(\eta^4+n^4+6\eta^2n^2q^2+n^4q^4) \\ -2(c_{11}-c_{13})(n^2q^2+\eta^2)^2n^4 \end{bmatrix}\times\right.$$
$$\times\frac{b_{14}(\eta^4+n^4+6\eta^2n^2q^2+q^4n^4)+2(b_{13}-b_{32})(n^2q^2+\eta^2)n^2+(q^2n^2+\eta^2)r}{b_{11}(\eta^4+n^4+6\eta^2n^2q^2+q^4n^4)+2(b_{12}+b_{31})(n^2q^2+\eta^2)n^2}+$$
$$+c_{13}(6\eta^2n^2q^2+\eta^4+n^4+q^4n^4)+2(c_{14}+c_{32})(n^2q^2+\eta^2)n^2+$$
$$\left.+\left[K_1+K_2(q^2n^2+\eta^2)\right]r^2\right\} \qquad 16)$$

where $\eta=\pi r/a$.

At $K_2=0$ in expression (16), the expression for the critical torsional load of the cylindrical shells formed from FGMs on the Winkler soil is obtained.

At $K_1=K_2=0$ in expression (16), the expression for the unconstrained critical torsional load of the cylindrical shells made of FGMs is obtained.

5. Results and discussion

5.1. Comparison

In table 1, the magnitudes of the critical torsional load of unconstrained cylindrical shells made of FGMs for different r/t ratios are compared with the results of the Huang and Han [12]. It is considered that here $S_{cr}=M_{cr}/(2\pi r^2t)$. FGM, which consists of a ceramic-metal mixture, consists of a mixture of zirconium (ZrO_2) and titanium-alloy (Ti_6Al_4V). Young's modulus and Poisson's ratio of metal (ZrO_2) and ceramic (Ti_6Al_4V) materials are as follows: $E^c=1.68063\times10^5$ MPa, $E^m=1.05698\times10^5$ MPa, $v^c=0.297996$ and $v^m=0.298096$ [18]. The thickness of the cylindrical shells made of FGMs is $t=0.001$m, $a/r=2$ and the variation of the r/t ratio is presented in table 1. These data were taken from Huang and Han [12]. Numbers in parentheses indicate critical torsion load values. Although the minimum values of the critical torsional load are different (q, n), the values of the critical torsional load are in good agreement.

5.2. Specific analysis

The cylindrical shells used in this section consist of pure metal, pure ceramic and FGM, which is a mixture of them. As FGM, it is a mixture of zirconium (ZrO_2) and titanium-alloy, and its properties are shown above. The analysis considers three different FGM profiles. In figures 2-4, the variations of Young's modulus with respect to the dimensionless thickness coordinate Z for the volume fraction $k=0.25$, $k=0.5$ and $k=1$, respectively, are shown in three dimensions using the Maple 13 program based on the relation (3). The vertical axis is taken into account as $\bar{E}^{Fd}=E^{Fd}(Z)/10^{11}$ (Pa), $X=x/t$ and $Z=z/t$ are dimensionless coordinates.

The values of the critical torsion moment in numerical calculations are written $M_{cr}/100$ as in the subsequent tables. The changes of the critical torsional moment (M_{cr}) of fully ceramic, FGM (or Ti_6Al_4V/ZrO_2) and fully metal cylindrical shells depending on the elastic soil coefficients K_1 and K_2 are presented in table 2. The volume fraction and the geometric data are considered as: $k=0.5$, $r/t=100$ and $a/r=2$. As can be seen from table 2, the magnitudes M_{cr} for pure ceramic, FGM with the volume fraction index $k=0.5$ and pure metal cylindrical shells increase depending on the increase of the K_1 and K_2. Depending on the increase of the K_1 and K_2, the

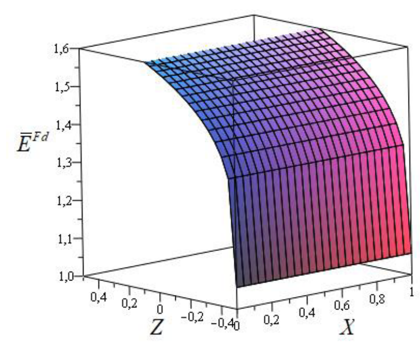

Fig.2. Three dimensions distributions of $\bar{E}^{Fd}=E^{Fd}(Z)/10^{11}$ for the volume fraction index $k=0.25$

Table 1

Comparison of the values of critical torsional load of cylindrical shells made of FGMs with the study of Huang and Han [12]

	S_{cr} (MPa), (q, n)	
r/t	Huang and Han [12]	Present Study
300	48.61 (11, 0.33)	49.86 (9, 0.22)
400	33.82 (12, 0.31)	34.44 (10, 0.21)
500	25.58 (13, 0.30)	25.93 (11, 0.20)

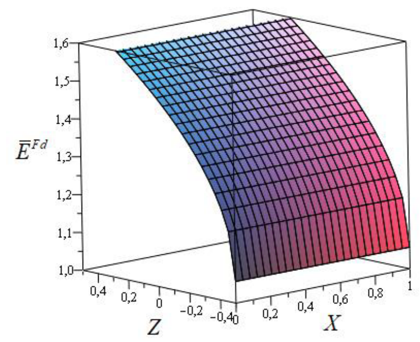

Fig.3. Three dimensions distributions of $\bar{E}^{Fd} = E^{Fd}(Z)/10^{11}$ for the volume fraction index k = 0.5

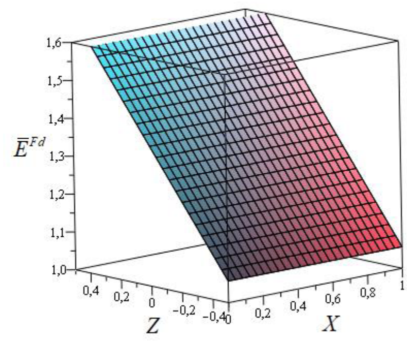

Fig.4. Three dimensions distributions of $\bar{E}^{Fd} = E^{Fd}(Z)/10^{11}$ for the volume fraction index k = 1

n wave numbers remain almost constant, while the values of the q vary between 0.3 and 0.41 and generally increase. As can be seen from table 2, while the largest values of M_{cr} are obtained for pure ceramic and its smallest value for pure metal, while those decrease from pure ceramic to pure metal in FGM cylindrical shells. When the FGM profile is compared with pure ceramic shell, the influence of the FGM on the critical torsional moment of the unground cylindrical shell is (-10.8%). This effect decreases depending on the increase of the K_1 and K_2. For example, when $K_2 = 0$, the effect of FGM on the M_{cr} decreases by around (+1.0%) depending on the increase of the K_1 from 0 to 2×10^7. In addition, the FGM effect decreases approximately (+1.1%) depending on the increase of the $K_1 = 2\times10^7$ and K_2 from 0 to 1.4×10^5. The influence of FGM on the critical torsional moment of unground cylindrical shells is (+42.4%), when the FGM profile is compared with the pure metal. This effect decreases depending on the increase of the K_1 and K_2 . For example, when $K_2 = 0$, the FGM effect decreases (+7%) depending on the increase of the K_1 from 0 to 1.5×10^7. In addition, the FGM effect (+3.6%) decreases depending on the increase of the K_2 from 0 to 1.4×10^5 at $K_1 = 1.5\times10^7$. The effect of elastic soil on the values of M_{cr} for cylindrical shells increases with the increase of K_1 and K_2. For example, when $K_2 = 0$, due to the increase of K_1 from 1×10^7 to 2×10^7, the Winkler ground effect on the M_{cr} of cylindrical shells made of pure ceramic, FGM and pure metal increase from (+12.7%) to (+22.2%), from (+14.2%) to (+23.4%) and from (+19.2%) to (+32.3%), respectively. When $K_1 = 1.5\times10^7$, depending on the increase of K_2 from 8×10^4 to 1.4×10^5, the Pasternak-type ground effect on the of cylindrical shells increase from (+22.8%) to (+26.6%), from (+24.8%) to (+29.1%) and from (+33.3%) to (+39.4%), for the pure ceramic, the FGM and the pure metal cases, respectively.

The variations of the magnitudes of M_{cr} for cylindrical shells made of pure ceramic, pure metal and FGM with the volume fraction index k = 0.25; 0.5; 1.0 depending on the a/r ratio are presented in Table 3 in the presence and absence soils at r/t = 100. As can be seen from table 3, the values of M_{cr} decrease in pure metal (Ti_6Al_4V) and pure ceramic (ZrO_2) and FGM profiles depending on the increase of a/r. In addition, while the wave number n remains constant in the range of $a/r > 2$, it decreases in the range of $a/r \le 2$. While the parameter q decreases for ungrounded FGM cylindrical shells depending on the increase of the a/r, it remains constant in the range of $a/r > 2$ for grounded FGM cylindrical shells. When FGM cases are compared among themselves, the largest M_{cr} value occurs at $k = 0.25$ and the smallest M_{cr} value occurs at $k = 1$. When the FGM cases are compared to the pure ceramic case, the FGM effect remains almost constant in the ungrounded condition due to the increase of the a/r, while it decreases in the grounded cases. When FGM cases are compared among themselves, the largest FGM effect is obtained for $k = 1$ and the smallest FGM effects obtained for $k = 0.25$. For example, depending on the increase of a/r from 0.5 to 3, the effect of FGM on M_{cr} decreases from (-18.4%) to (-16.1%) in the case of Winkler soil, whereas it decreases from (-17.6%) to (-14.7%) for $k = 1$. It remains almost constant at (-18.5%) without ground. When $a/r = 3$, the largest FGM effect difference between cases $k = 0.1$ and $k = 0.5$ is approximately (+8%), and the largest FGM effect difference between cases $k = 0.25$ and $k = 1$ is approximately (+12%). When the FGM cases is compared to the pure metal case, the FGM effect remains almost constant in the unground condition, while decreasing in the grounded condition, due to the increase of the a/r. When FGM cases are compared among themselves, the smallest FGM effect is obtained for $k = 1$ and the largest FGM effect is obtained for $k = 0.25$. For example, for $k = 0.25$, due to the increase of a/r from 0.5 to 3, the effect of FGM on M_{cr} values decreases from (48.9%) to (40%) in the presence of Winkler ground, while from (+45.9%) to (+34.1%) in the presence of Pasternak ground. In the groundless condition the effect is (+49.5%), it remains almost constant. When $a/r = 3$, the largest FGM effect difference between cases $k = 0.25$ and $k = 0.5$ is approximately (+8%), and the largest FGM effect difference between $k = 0.25$ and $k = 1$ cases is approximately (+20%). The Pasternak and Winkler elastic grounds effect on M_{cr} values of cylindrical shells with homogeneous and FGM profiles increases depending on the increase of a/r. The largest ground effects are obtained in pure metal and the smallest ground effects are obtained in pure ceramic shells. For example, the values of M_{cr} in pure metal cylindrical shells increase from (+1.5%) to (+32.9%) for Winkler ground and increase from (+8.2%) to (+59.5%) for Pasternak-type ground due to the increase of a/r from 0.5 to 3. The greatest Winkler ground effects between pure metal case and FGMs with profiles k = 0.25; 0.5; 1.0 and pure ceramic cases are obtained as (+8.3%), (+7%), (+5.5%) and (+9.9%), respectively, whereas the greatest Pasternak-type soil effects are obtained as (+16.3%), (+14.9%), (+11.5%) and (+19%), respectively, at $a/r = 3$.

Table 2

Variation of critical torsional moment (M_{cr}) of cylindrical shells made of pure ceramic, FGM and pure metal depending on the ground coefficients K_1 and K_2

		$M_{cr}/100$, (q, n)		
K_2	K_1	ZrO_2	FGM(k = 0.5)	Ti_6Al_4V
0	0	0.158 (0.3, 7)	0.141 (0.3, 7)	0.099 (0.3, 7)
0	1.0×10^7	0.178 (0.33, 7)	0.161 (0.33, 7)	0.118 (0.37, 8)
	1.5×10^7	0.186 (0.37, 8)	0.168 (0.37, 8)	0.124 (0.38, 8)
	2.0×10^7	0.193 (0.38, 8)	0.174 (0.38, 8)	0.131 (0.4, 8)
0.8×10^5	1.0×10^7	0.187 (0.33, 7)	0.169 (0.37, 8)	0.126 (0.38, 8)
	1.5×10^7	0.194 (0.38, 8)	0.176 (0.38, 8)	0.132 (0.39, 8)
	2.0×10^7	0.2 (0.38, 8)	0.182 (0.39, 8)	0.138 (0.41, 8)
1.1×10^5	1.0×10^7	0.19 (0.34, 7)	0.172 (0.38, 8)	0.129 (0.39, 8)
	1.5×10^7	0.197 (0.38, 8)	0.179 (0.38, 8)	0.135 (0.4, 8)
	2.0×10^7	0.203 (0.39, 8)	0.185 (0.39, 8)	0.141 (0.41, 8)
1.4×10^5	1.0×10^7	0.193 (0.34, 7)	0.175 (0.38, 8)	0.131 (0.39, 8)
	1.5×10^7	0.2 (0.38, 8)	0.182 (0.39, 8)	0.138 (0.4, 8)
	2.0×10^7	0.206 (0.39, 8)	0.188 (0.39, 8)	0.144 (0.41, 8)

Table 3

Variations of the values of for cylindrical shells made of pure metal, pure ceramic and various FGM profiles depending on the ratio with and without elastic soils

		$M_{cr}/100$, (q, n)				
	a/r	Ceramic	FGM			Metal
		ZrO_2	k = 0.25	k = 0.5	k = 1	Ti_6Al_4V
$M_{cr}/100, (q, n)$	0.5	0.426 (0.58, 11)	0.448 (0.6, 11)	0.38 (0.58, 11)	0.347 (0.58, 11)	0.268 (0.58, 11)
	1	0.243 (0.43, 9)	0.27 (0.46, 9)	0.216 (0.43, 9)	0.198 (0.43, 9)	0.153 (0.43, 9)
	1.5	0.187 (0.36, 8)	0.221 (0.39, 8)	0.167 (0.36, 8)	0.153 (0.36, 8)	0.118 (0.36, 8)
	2	0.158 (0.3, 7)	0.199 (0.38, 8)	0.141 (0.3, 7)	0.128 (0.3, 7)	0.099 (0.3, 7)
	2.5	0.14 (0.26, 6)	0.185 (0.34, 7)	0.124 (0.26,6)	0.114 (0.26, 6)	0.088 (0.26, 6)
	3	0.126 (0.25, 6)	0.177 (0.34, 7)	0.112 (0.25, 6)	0.102 (0.25, 6)	0.079 (0.25, 6)
$M_{cr}^{w}/100, (q, n)$	0.5	0.43 (0.59, 11)	0.405 (0.59, 11)	0.384 (0.59, 11)	0.351 (0.59, 11)	0.272 (0.59, 11)
	1	0.252 (0.44, 9)	0.237 (0.44, 9)	0.225 (0.44, 9)	0.207 (0.44, 9)	0.162 (0.45, 9)
	1.5	0.201 (0.37, 8)	0.19 (0.37, 8)	0.181 (0.37, 8)	0.166 (0.38, 8)	0.131 (0.38, 8)
	2	0.178 (0.33, 7)	0.169 (0.33, 7)	0.161 (0.33, 7)	0.149 (0.37, 8)	0.118 (0.37, 8)
	2.5	0.163 (0.32, 7)	0.155 (0.32, 7)	0.148 (0.32, 7)	0.137 (0.33, 7)	0.11 (0.33, 7)
	3	0.155 (0.32, 7)	0.147 (0.32, 7)	0.141 (0.32, 7)	0.13 (0.33, 7)	0.105 (0.33, 7)
$M_{cr}^{wp}/100, (q, n)$	0.5	0.448 (0.6, 11)	0.423 (0.6, 11)	0.402 (0.6, 11)	0.369 (0.6, 11)	0.29 (0.61, 11)
	1	0.27 (0.46, 9)	0.256 (0.46, 9)	0.244 (0.46, 9)	0.225 (0.46, 9)	0.18 (0.47, 9)
	1.5	0.221 (0.39, 8)	0.21 (0.39, 8)	0.2 (0.4, 8)	0.186 (0.4, 8)	0.151 (0.41, 8)
	2	0.199 (0.38, 8)	0.189 (0.38, 8)	0.181 (0.38, 8)	0.168 (0.39, 8)	0.137 (0.4, 8)
	2.5	0.185 (0.34, 7)	0.176 (0.34, 7)	0.169 (0.35, 7)	0.158 (0.35, 7)	0.131 (0.36, 7)
	3	0.177 (0.34, 7)	0.169 (0.34, 7)	0.162 (0.34, 7)	0.151 (0.35, 7)	0.126 (0.36, 7)

Conclusion

In this study, the analytical solution of the buckling problem of cylindrical shells consisting of FGMs on the Pasternak-type elastic soil under the torsional moment is discussed. First, linear basis relations of cylindrical shells made of FGMs are established using the Donnell type shell theory. Using these relations and the mathematical model of the Pasternak-type elastic soil, the fundamental partial differential equations of cylindrical shells composed of FGMs under torsional moment are derived. In the next step, the basic equations are solved by applying Galerkin's method, and a closed form solution is obtained for the critical torsional moment of cylindrical shells consisting of FGMs on the Pasternak-type elastic soil. Numerical analyzes reveal that the effects of volume fraction and soil coefficients on the critical torsional moment are significant.

References

1. Koizumi, M. (1993). The concept of FGM. *Ceramic Transactions, Functionally Gradient Materials*, 34, 3–10.

2. Lannutti, J. (1994). Functionally graded materials: properties, potential and design guidelines. *Composites Engineering*, 4, 81-94.

3. Leushake, U., Krell, T., Schulz, U. (1997). Graded thermal barrier coating systems for gas turbine applications. *Materialwissenschaften und Werkstofftechnik*, 28, 391-394.

4. Zoltan, K., Bela, V. (2012). Processing of functionally graded aluminium alloys. *Metalurgia International*, 17, 22-26.

5. Torres, Y., Trueba, P., Pavon Palacio, J., et al. (2016). Design, processing and characterization of titanium with radial graded porosity for bone implants. *Materials & Design*, 110, 179-187.

6. Pelz, J., Ku, N., Shoulders, W., et al. (2020). Multi-material additive manufacturing of functionally graded carbide ceramics via active, in-line mixing. *Additive Manufacturing*, 37, 101647.

7. Suethao, S., Shah, D., Smitthipong, W. (2020). Recent progress in processing functionally graded polymer foams. *Materials*, 13, 4060.

8. Lee, N., Weber, R., Kennedy, J., et al. (2020). Sequential multimaterial additive manufacturing of functionally graded biopolymer composites. *3D Printing and Additive Manufacturing*, 7, 205-215.

9. Vasavi, B., Raghavendra, D. G., Ojha, S., et al. (2021). State of the art in functionally graded materials. *Composite Structures*, 262, 113596.

10. Madan, R., Bhowmick, S. (2020). A review on application of FGM fabricated using solid-state processes. *Advances in Materials and Processing Technologies*, 6, 608-619.

11. Sofiyev, A. H., Schnack, E. (2004). The stability of functionally graded cylindrical shells under linearly increasing dynamic torsional loading. *Engineering Structures*, 26, 1321-1331.

12. Huang, H. W., Han, Q. (2010). Nonlinear buckling of torsion–loaded functionally graded cylindrical shells in thermal environment. *European Journal Mechanics A-Solids*, 29, 42–48.

13. Sun, J., Xu, X., Lim, C. W. (2013). Torsional buckling of functionally graded cylindrical shells with temperature-dependent properties. *International Journal of Structural Stability and Dynamics*, 14, 1350048.

14. Shen, H.-S. (2014). Torsional postbuckling of nanotube-reinforced composite cylindrical shells in thermal environments. *Composite Structures*, 116, 477–488.

15. Sofiyev, A. H., (2019). Review of research on the vibration and buckling of the FGM conical shells. *Composite Structures*, 211, 301-317.

16. Sun, J., Ni, Y., Hanyu, G., et al. (2019). Torsional buckling of functionally graded multilayer graphene nanoplatelet-reinforced cylindrical shells. *International Journal of Structural Stability and Dynamics*, 20, 2050005.

17. Soltani, M., Asgarian, B. (2020). Lateral-torsional stability analysis of a simply supported axially functionally graded beam with a tapered i-section. *Mechanics of Composite Materials*, 56, 39-54.

18. Shen, H. S. (2009). Functionally graded materials, nonlinear analysis of plates and shells. *Florida: CRC Press*.

19. Kerr, A. D. (1964). Elastic and visco-elastic foundation models. *Journal of Applied Mechanics*, 31, 491–498.

20. Pasternak, P. L. (1954). On a new method of analysis of an elastic foundation by means of two foundation constants. *Moscow: State Publishing House Building and Architecture Literature*.

21. Vlasov, V. Z., Leont'ev, N. N. (1966). Beams, plates and shells on elastic foundations. *Translated from Russian to Enghlish by Barouch, A, Israel Program for scientific translations, Jarusalem*.

22. Bajenov, V. A., (1975). The bending of the cylindrical shells in an elastic medium. *Kiev: Visha Shkola*.

23. Dung, D., Hoa, L. (2015). A semi-analytical approach to analyze the nonlinear dynamic torsional buckling of stiffened FGM circular cylindrical shells surrounded by elastic medium. *Applied Mathematical Modelling*, 39, 6951-6967.

24. Dung, D., Hoa, L. (2015). Nonlinear torsional buckling and postbuckling of eccentrically stiffened FGM cylindrical shells in thermal environment. *Composites Part B: Engineering*, 69, 378-388.

25. Ninh, D., Bich, D., Bui, H. (2015). Torsional buckling and post-buckling behavior of eccentrically stiffened functionally graded toroidal shell segments surrounded by an elastic medium. *Acta Mechanica*, 226, 3501-3519.

26. Ninh, D., Bich, D. (2016). Nonlinear torsional buckling and post-buckling of eccentrically stiffened ceramic functionally graded material metal layer cylindrical shell surrounded by elastic foundation subjected to thermo-mechanical load. *Journal of Sandwich Structures and Materials*, 18, 712-738.

27. Nam, V., Phuong, N., Minh, K., Hiếu, P. (2018). Nonlinear thermo-mechanical buckling and post-buckling of multilayer FGM cylindrical shell reinforced by spiral stiffeners surrounded by elastic foundation subjected to torsional loads. *European Journal of Mechanics A/Solids*, 72, 393-406.

28. Sofıyev, A. H., Yenialp, R. (2021, December). Analysis of the elastic foundation effect on buckling of functionally graded cylindrical shells under torsional load. *Proceeding of International scientific-practical conference «Machine-building and energy: new concepts and technologies». Baku, Azerbaijan: Azerbaijan Technical University*.

29. Sofiyev, A. H., Kuruoglu, N. (2022). Buckling analysis of shear deformable composite conical shells reinforced by CNTs subjected to combined loading on the two-parameter elastic foundation. *Defence Technology*, 18(2), 205-218.

30. Volmir, A. S., (1967). The stability of deformable systems. *Moscow: Nauka*.

О критическом крутящем моменте цилиндрических оболочек из функционально-градированных материалов (FGM), опирающихся на грунт типа Пастернака

А. Г. Софиев[1], Ф. Кадыоглу[2], И. А. Халилов[3], Г. М. Седихи[4], Т. Вергул[2], Р. Йениалп[1]
[1]Университет им. Сулеймана Демиреля, Испарта, Турция; [2]Истанбулский технический университет, Стамбул, Турция; [3]Азербайджанский технический университет, Баку, Азербайджан; [4]Ахвазский университет им. Шахид Камрана, Ахваз, Иран; [5]UNEC Азербайджанский государственный экономический университет, Баку, Азербайджан;
[6]Стамбульский университет коммерции, Стамбул, Турция

Реферат

В данной работе выполнен расчет на устойчивость цилиндрических оболочек из функционально-градированных материалов (FGM) под действием крутящего момента, опирающихся на грунт типа Пастернака. После установления линейных определяющих соотношений цилиндрических оболочек из FGM в рамках модифицированной теории оболочек типа Доннелла выводятся основные уравнения цилиндрических оболочек из FGM под действием крутящего момента с учетом влияния грунта типа Пастернака. Аналитическая формула для крутящего момента получена выбором аппроксимационных функций, удовлетворяющих граничным условиям в интегральном смысле. Из полученной формулы как частный случай получаются формулы для критического крутящего момента при наличии грунта Винклера и при отсутствии грунта. Подробно исследованы изменения критического крутящего момента для различных коэффициентов грунта, отношения объемной доли и характеристик оболочки.

Ключевые слова: функционально-градированные материалы; цилиндрическая оболочка; продольный изгиб; критический крутящий момент; грунт типа Пастернака.

Pasternak tipli qruntda yerləşən funksional qradasiyalı materiallardan (FGM) hazırlanmış silindrik örtüklərin böhran burucu momenti haqqında

A. H. Sofiyev[1], F. Kadıoğlu[2], İ. Ə. Xəlilov[3], H. M. Sedighi[4], T. Vergul[2], R. Yenialp[1]
[1]Suleyman Demirel Universiteti, Isparta, Turkiyə; [2]Istanbul Texniki Universiteti, Istanbul, Turkiyə; [3]Azərbaycan Texniki Universiteti, Bakı, Azərbaycan; [4]Ahvaz Shahid Chamran Universiteti, Ahvaz, Iran; [5]UNEC Azərbaycan Dövlət İqtisad Universiteti, Bakı, Azərbaycan;
[6]İstanbul Ticarət Universiteti, İstanbul, Türkiyə

Xülasə

Bu məqalədə Pasternak tipli qruntda yerləşən və burucu momentin təsiri altında olan funksional qradasiyalı materiallardan (FGM) hazırlanmış silindrik örtüklərin dayanıqlıq hesabatı aparılmışdır. Donnell tipli örtüklərin dəyişdirilmiş nəzəriyyəsi çərçivəsində FGM silindrik örtüklərinin xətti asılılıqları qurulduqdan sonra, Pasternak tipli qruntun təsirini nəzərə almaqla burucu momentin təsiri altında FGM silindrik örtüklərinin əsas tənlikləri alınmışdır. Burucu momentin analitik düsturu inteqral mənada sərhəd şərtlərini ödəyən yaxınlaşma funksiyaları seçməklə əldə edilmişdir. Xüsusi hal kimi alınmış ifadədən Vinkler qruntu üçün və qrunt olmayan hal üçün kritik burucu moment düsturları alınmışdır. Müxtəlif qrunt əmsalları, həcm nisbətləri və örtük xüsusiyyətləri üçün kritik burucu momentin dəyişməsi ətraflı tədqiq edilmişdir.

Açar sözlər: funksional qradasiyalı materiallar; silindrik örtük; uzununa əyrilik; kritik burucu moment; Pasternak tipli qrunt.